Materials Science and Engineering A 507 (2009) 194–199

Contents lists available at ScienceDirect

Materials Science and Engineering A

journal homepage: www.elsevier.com/locate/msea

Synthesis of multi-walled CNT reinforced aluminium alloy composite via friction stir processing

D.K. Lim [a], T. Shibayanagi [b], A.P. Gerlich [a,*]

[a] Chemical and Materials Engineering, University of Alberta, 536 CME Building, Edmonton, Alberta T6G 2G6, Canada
[b] Joining and Welding Research Institute (JWRI), Osaka University, Japan

ARTICLE INFO

Article history:
Received 15 October 2008
Accepted 30 November 2008

Keywords:
Friction stir processing
Carbon nanotubes
Metal matrix composite
Aluminium

ABSTRACT

Friction stir processing is used to produce an aluminium alloy reinforced with multi-walled carbon nanotubes. Microscopy by SEM and TEM indicates that the nanotubes are embedded into Al-alloy matrix produced in the stir zone, and their multi-walled microstructure survived the thermo-mechanical conditions imposed during processing. Increasing the tool rotation speed from 1500 and 2500 rpm and increasing the tool shoulder penetration depth improved homogeneity of nanotubes in the Al-alloy matrix, however a fully uniform distribution could not be achieved when regularly tangled nanotubes were used.

1. Introduction

The addition of carbon nanotubes (CNT) into various materials as a reinforcing fibre is a topic of much recent interest. In addition to good chemical and thermal stability, CNTs demonstrate high yield strength and elastic modulus values [1–6]. For example, single walled and multi-walled carbon nanotubes have elastic modulus of up to 1 TPa, and a yield strengths as high as 50 GPa [2,5]. As a result, these materials offer great potential as a reinforcing fibre in composite materials. Some success has already been achieved in incorporating CNTs into polymer and ceramic matrices [3], and a few studies have focused on the preparation of metal matrix composites (MMC) reinforced with CNTs [7–10]. In these composites there is evidence of poor interfacial bonding between the CNTs and the metal matrix [7], and this may be detrimental to the mechanical properties of these composites. Furthermore, agglomeration of the CNTs may produce an uneven dispersion within the matrix which reduces their effectiveness [8]. Potential damage of the nanotube structure, and chemical reactions with the matrix may also reduce the mechanical properties of these composites [7,9], as well as their orientation within the matrix [10]. These are all challenges that need to be addressed in optimizing the synthesis of CNT metal matrix composites.

With this in mind, a range of methods have been explored in previous research, including equal channel angular pressing (ECAP) [11], shockwave consolidation [12], and mechanical alloying [13], however some drawbacks have been revealed when each of these techniques are applied. Shockwave consolidation was found to produce a two-phase system liable to fail at stresses lower than bulk metal strength due to intergranular delamination [12]. Morsi and Esawi report that increased ball milling time improves the distribution of CNTs in the matrix, but also damages their structure [13]. Nanoscale dispersion, and molten methods involving squeeze casting provide slightly improved nanotube dispersion and mechanical properties, however a limited number of materials may be used for the matrix using these methods [14,15].

Friction stir processing (FSP) is a solid-state joining and microstructural modification process [16,17], where a rotating tool pin is plunged into the surface of the metals to be processed and traversed along its surface. The friction and plastic deformation imposed by the tool heats and softens the workpiece, and the tool pin promotes intermixing of material in a local region. When reinforcing particles are introduced into a hole or groove on the surface of the material in the path of the tool, they are dispersed throughout the stirred zone [18]. In contrast to other methods of producing CNT composites, FSP does not require multiple processing steps, rely on precursor metal powders, or involve melting [16–18]. FSP also has the added benefit of refining the grain size in the alloy matrix, and this effect is enhanced with the addition of CNTs as noted by Morisada et al. [8]. Single walled nanotubes have also been incorporated into Al 7075 alloy, however there was some evidence of broken nanotubes in the composite produced [19].

The present work focuses on using FSP as synthesis method for producing composite of Al alloys with multi-walled CNTs. The effect of the processing parameters of plunge depth and rotational speed on the microstructures and distribution of CNTs in the compos-

* Corresponding author. Tel.: +1 780 492 8853; fax: +1 780 492 2881.
E-mail address: gerlich@ualberta.ca (A.P. Gerlich).

0921-5093/$ – see front matter.
doi:10.1016/j.msea.2008.11.067

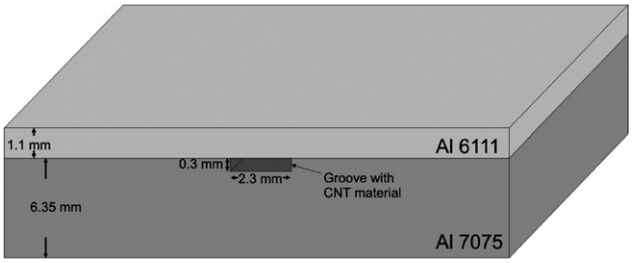

Fig. 1. Schematic of base material layout prior to friction stir processing.

Table 1
Base material compositions, in wt%.

Alloy	Al	Cr	Cu	Fe	Mg	Mn	Si	Zn
Al 6111–T4	Balance	<0.01	0.75	0.25	0.75	0.20	0.69	0.02
Al 7075–T6	Balance	0.21	1.27	0.12	2.34	<0.01	0.07	5.41

ite material are examined. To examine the effectiveness of friction stir process in dispersing the CNTs throughout the matrix, regularly tangled CNTs were used in this study without applying any prior agitation to disentangle them.

2. Experimental procedure

The composite materials were synthesized by encasing the multi-walled CNT powder in a 0.3 mm × 2.3 mm groove in a lower plate which was covered by a top sheet before friction stir processing, as shown in Fig. 1. A sheet of 1.1 mm thick Al 6111–T4 alloy was used as cover plate to contain the CNT material within the groove during processing, and the lower plate was 6.35 mm thick Al 7075–T6 alloy. The Al 6111–T4 and Al 7075–T6 base materials have an average microhardness of 95 HV and 180 HV, respectively. Table 1 indicates the base metal compositions of the plates used in the preparation of all four samples. These two alloys were employed to reveal the flow patterns created by the tool during processing when examined by optical microscopy following etching. The CNT base material had outer diameters of 30–50 nm, and were 10–20 μm in length, see Fig. 2. The CNT material used in this study was regularly tangled in order to determine the effectiveness of friction stir processing in dispersing the CNTs throughout the Al-alloy matrix.

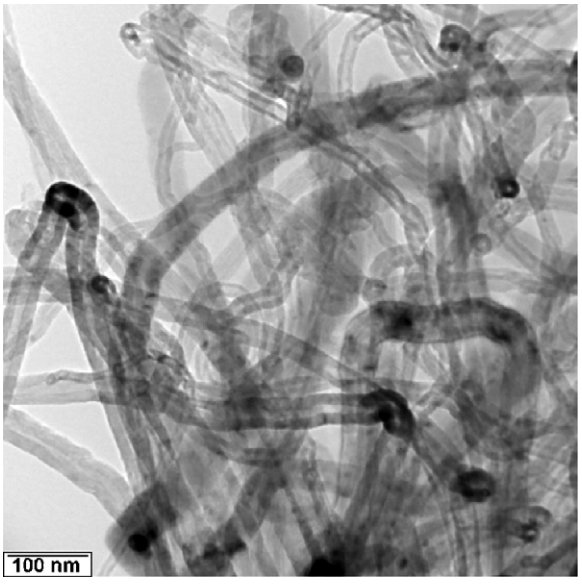

Fig. 2. TEM micrograph of the multi-walled CNT material.

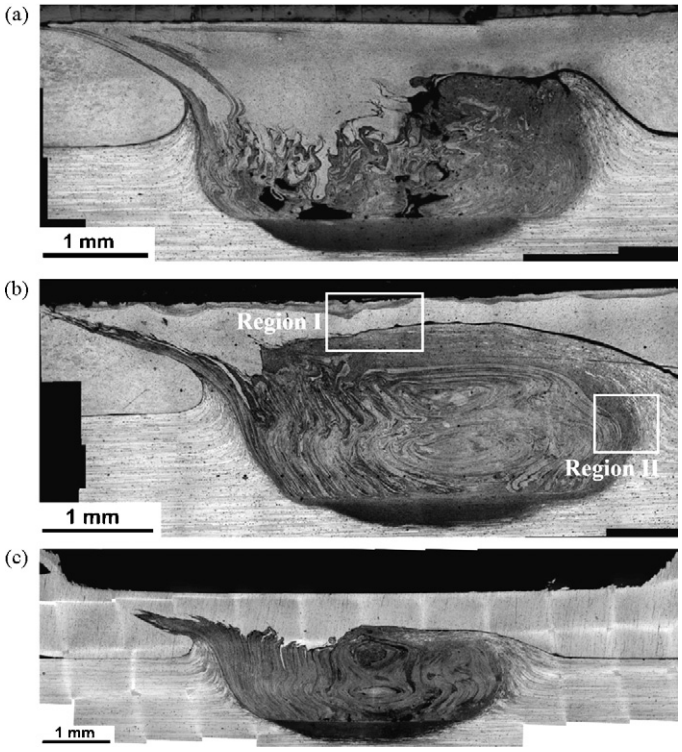

Fig. 3. Optical micrographs of friction stir processed regions processed with (a) 1500 rpm and 0.03 mm of shoulder penetration, (b) 1500 rpm and 0.24 mm of shoulder penetration and (c) 2500 rpm and 0.24 mm of shoulder penetration.

All samples were processed using a tool consisting of a cylindrical 10 mm diameter shoulder and a 4 mm diameter, 2.2 mm long pin with an M4 metric thread profile. The tool was rotated counterclockwise when viewed from above to promote downward flow of material in the sheets, and linearly traversed at 2.5 mm/s. The rotational speeds were 1500–2500 rpm, and the shoulder penetrated into the upper sheet of Al 6111 by 0.03–0.24 mm. It should be noted that although a simple threaded tool does not produce an optimum bond between overlapping sheets [20], this geometry was selected in order to simplify the analysis of the complex material flow produced during friction stir welding [21].

Transverse sections were examined by optical and electron microscopy and etched using Keller's reagent (1 ml 48% HF, 1.5 ml HCl and 10 ml nitric acid in 87.5 ml distilled water) for 30 s. Scanning electron microscopy with a Hitachi S-2700 SEM and a JEOL 6301F FESEM was used to examine the cross-sections. The structure of the CNT base material as well as those embedded within the Al-alloy matrix was examined using a JEOL 2010 TEM operating at 200 keV. TEM samples were prepared by twin-jet electropolishing in a solution of 25 vol.% of HNO_3 and 75 vol.% of methanol at a temperature of −30 °C and a voltage of 12 V. The Vickers microhardness of the material was measured with a Mitutoyo MVK-H1 indenter using a 50 or 100 g load and 10 s loading time.

3. Results and discussion

3.1. Effect of processing parameters

Optical micrographs of the friction stir processed materials are shown in Fig. 3. Contrast between the Al 6111 and Al 7075 material is clearly evident within the stir zones following etching, revealing complex flow patterns produced by intermixing of the upper and lower sheets. When a tool rotation speed of 1500 rpm and shoulder penetration of 0.03 mm was used, extensive voids were produced

in the stir zone with negligible intermixing of the two alloys, with only some of the Al 6111 being transferred downwards into the Al 7075 plate, see Fig. 3(a).

When a tool rotation speed of 1500 rpm is used and the shoulder penetration depth is increased to 0.24 mm, the stir zone is free of voids, see Fig. 3(b). The stir zone comprised lamellae of intermixed layers of Al 6111 and Al 7075 material. Although increasing the shoulder penetration depth prevented void formation in the stir zone, unbonded regions or fissures could still be observed between lamellae in the central region of the stir zone.

Increasing the tool rotation speed to 2500 rpm and the shoulder penetration depth to 0.24 mm reduced the thickness of the lamellae, making individual layers difficult to resolve as shown in Fig. 3(c). The bonding between the upper and lower sheet materials was incomplete for all processing parameters examined, as may be expected when joining overlapping sheets using a simple threaded tool [20]. The advancing side corresponds with the side where the direction of tool rotation is the same as the linear direction, which is the left side of the stir zones shown in Fig. 3, and bonding was mainly produced in this location of the weld.

In each of the welds in Fig. 3, a dark region was apparent at central lower region of each friction stir zone, which had a maximum thickness of 0.3 mm at the weld centreline. This region has been referred to as the vortex swirl zone [22], and is produced by the material flow immediately adjacent to the bottom surface of the tool pin. In the micrographs shown in Fig. 3, this region consistently occurs 2.2 mm below the top surface, which corresponds with the 2.2 mm pin length of the tool used in this study. It has been shown that a dynamically quiescent layer of material is established in this region immediately below the pin [23]. It was found that dynamically recrystallized grains are formed in this region, however material flow in the radial direction is only on the order of micrometers per second. As a result, no intermixed lamellae are produced below the pin.

The complex intermixing in the friction stir processed material has been widely observed during friction stir welding of dissimilar materials [24–26], and is more pronounced when higher tool rotation speeds are used [26–30]. It has been shown that the intermixing of dissimilar alloys during friction stir welding occurs as a result of the downward flow of material produced by the threads [23,30]. It has also been shown that alternating lamellae of the two materials are produced by a helical flow upwards when the material exits the thread feature on the bottom of the rotating pin [24,30]. Since a ribbon of dissimilar Al 6111 and Al 7075 lamellae is discharged with each tool rotation, the thickness of the lamellae will decrease with tool rotation speed if the stir zone volume remains constant [29]. This accounts for the increase in the number of lamellae and decrease in their thickness when the tool rotation speed was increased from 1500 to 2500 rpm in Fig. 3(b) and (c).

Fig. 4. SEM backscattered electron micrograph lamellae in the stir zone of seam weld produced using 2500 rpm and tool penetration of 0.24 mm. EDX analysis from location A was 86.2% Al, 9.5% Zn, 2.8% Cu, 1.5% Mg, and location B was 97.2% Al, 1.7% Cu, 0.6% Zn, 0.5% Mg, all in wt%.

The lamellae formed within the stir zone produced during intermixing via the pin threads are shown in Fig. 4. The EDX results indicate that the light regions (see location A in Fig. 4) correspond with Zn-rich regions originating from the Al 7075 base material, and dark regions corresponding with Al 6111 which were depleted in Zn. These results also indicate that limited inter-diffusion of the top and bottom alloy sheets occurred during friction stir processing, and that the lamellae were produced by mechanical intermixing of the two alloys via the threads on the tool pin [30].

3.2. CNT distribution and survivability

Fissures or unbonded regions were produced at the interface between some of the intermixed lamellae in Fig. 4. These fissures contained a large number of tangled CNTs which were not embedded in the Al-alloy matrix, see Fig. 5. In contrast the CNTs located within lamellae produced in the stir zone were embedded within the matrix, however their structure could only be clearly revealed following etching, see Fig. 6. The regions adjacent to the lamellae in Fig. 6 contained a higher concentration of CNT material, which was revealed more clearly following preferential etching of the dissimilar Al-alloy matrix. These results indicate that the long and entangled CNTs are not uniformly dispersed throughout the fric-

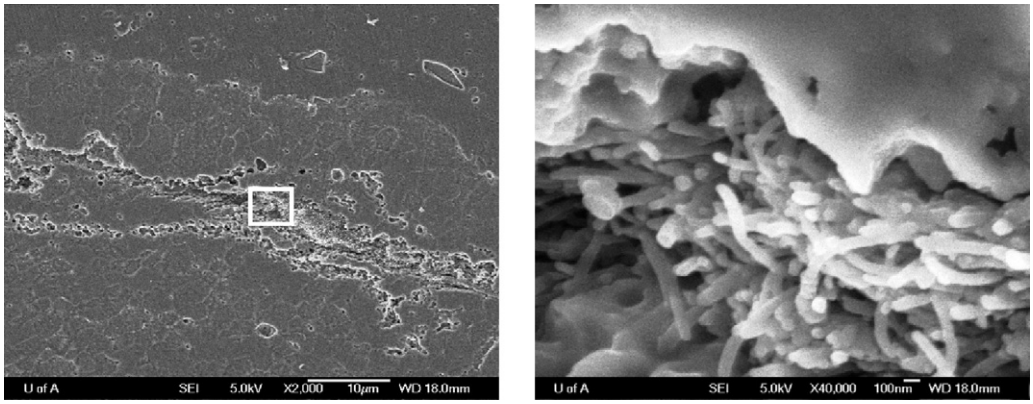

Fig. 5. SEM micrograph of a fissure located in the stir zone of seam weld produced using 2500 rpm and tool penetration of 0.24 mm, and high magnification image of CNT material found within the fissure.

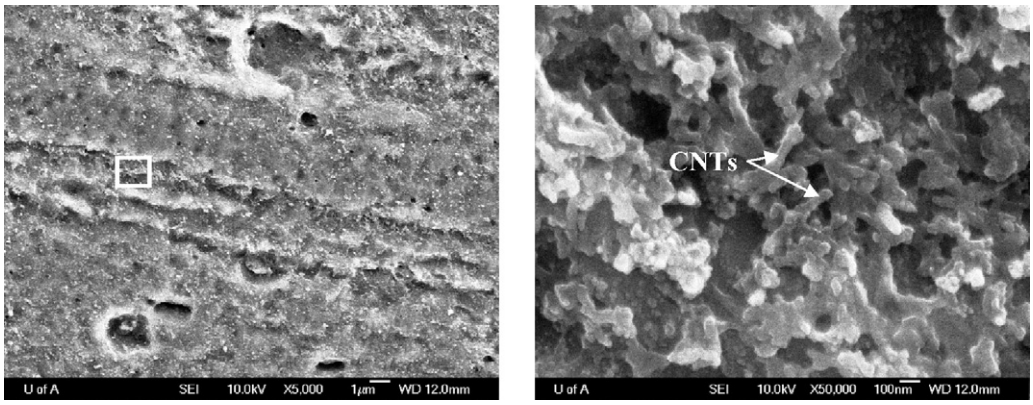

Fig. 6. SEM micrograph of lamellae located in the stir zone of seam weld produced using 1500 rpm and tool penetration of 0.24 mm, with CNT material embedded within the alloy matrix shown at high magnification.

tion stir processed region using parameters examined in the present study. Considering the nominal length of the nanotubes in the CNT base material was 10–20 μm, the significant number of open ends shown in Figs. 5 and 6 suggest that nanotubes may have fractured. However, this may have occurred during sample preparation.

TEM micrographs of the composite material in the stir zone indicate that the CNTs embedded within the Al-alloy matrix maintained their structure, see Fig. 7. The CNTs observed in the TEM micrograph are highly agglomerated, similar to those observed by SEM. The measured *d*-spacing values for the electron diffraction rings shown in Fig. 7 were 3.39, 2.07, and 1.19 Å, respectively. The Miller indices in Fig. 7 have been determined based on the hexagonal unit cell suggested by Keller et al. [31]. The first and most intense ring corresponds well with the reflection observed for the interlayer spacing found in multi-walled CNTs (3.478 Å) [31], and is close to the interplanar spacing found in graphite (3.35 Å) [32,33]. These results indicate that the multi-walled structure of the CNTs remained intact during the thermo-mechanical cycle imposed by friction stir processing.

3.3. Microhardness measurements

The highest microhardness values were observed when a tool rotation speed of 1500 rpm was used with 0.24 mm of shoulder penetration, in the location below the Al 6111 sheet interface. In Al 6111–T4 alloy, the average hardness in the stir zone following natural aging was 95 HV, which is similar to the base material which was also in a naturally aged condition. In the Al 7075–T6 alloy the typical hardness was 140 HV, which is much lower than the initial hardness in the peak-aged condition. This reduction already been explained by dissolution of precipitates in the stir zone [34]. For example, Al 7075 material friction stir processed using tool rotation speeds of 1500–3000 rpm had similar hardness values [35]. The location where the peak hardness value was obtained is shown in Fig. 8(a) and corresponded with value of 213 HV. This increase in hardness is accounted for by the presence of CNTs embedded in the Al-alloy matrix. The microhardness values in the boundary between the stir zone and the thermo-mechanically affected zone (TMAZ) the retreating side of the stir zone in all samples were also higher than the values within the intermixed material adjacent to this region, see Fig. 8(b). This suggests that the CNTs were not uniformly dispersed during friction stir processing.

Due to the tendency for CNT material to segregate along the lamellae regions in the stir zone, non-uniform hardness values were observed across the stir zone. The tendency for reinforcing particles to segregate preferentially in different locations in the stir zone has also been observed when friction stir processing Al-alloy/SiC composite materials [36]. It was observed that at higher rotation speeds, the SiC was distributed more preferentially along the outer edge of the stir zone and that the uniformity of the distribution was improved when multiple passes are applied. In contrast, friction stir processing of the Al with CNTs improved homogeneity when the rotation speed increased from 1500 to 2500 rpm due to the increase in the number of lamellae produced when friction stir processing using a single pass. It is likely that a more homogeneous distribution could be achieved with repeated passes without significantly degrading the multi-walled structure of the CNTs.

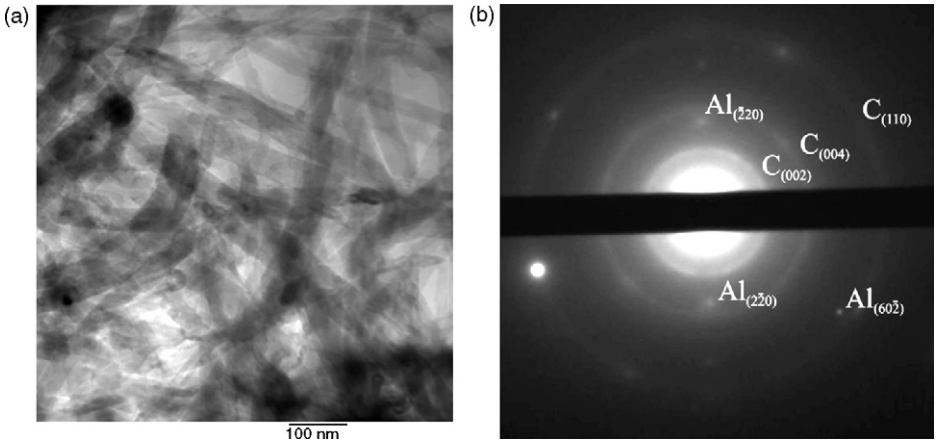

Fig. 7. (a) TEM image of CNTs embedded in Al matrix and (b) corresponding diffraction pattern along the Al {3 1 1} zone axis.

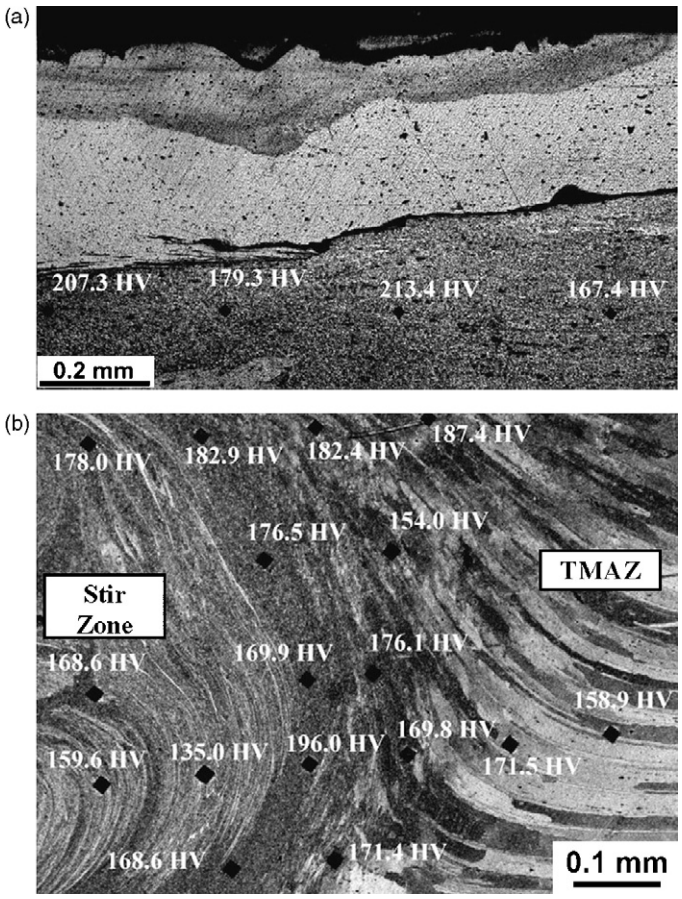

Fig. 8. Optical micrographs and hardness values in (a) Region I and (b) Region II in a sample produced using 1500 rpm, and a 0.24 mm plunge depth.

The microhardness values produced in a sample friction stir processed using 2500 rpm and a shoulder penetration depth of 0.24 mm is shown in Fig. 9. Since the stir zone consists of intermixed Al 6111 and Al 7075 alloys, one may expect that hardness values in the stir zone should be comparable to those produced in friction stir welded material of each of the alloys, ranging from 95 to 140 HV. However, regions in the stir zone are found where the microhardness exceeds these values, which suggests reinforcement by CNT material. Areas with values lower than 140 HV in Fig. 9 correspond with lamellae rich in Al 6111 material transferred downwards by the pin. The hardness across the bottom central region of the stir zone (line C–C) had a more uniform hardness compared to the bulk of the stir zone, with an average value around 170 HV, see Fig. 9. It is suggested that CNTs transferred downwards to this bottom region of the stir zone by the pin threads and was concentrated there due to the dynamically quiescent layer present under the pin [23], and this produces hardness values that are higher than those observed in friction stir processed Al 7075 material.

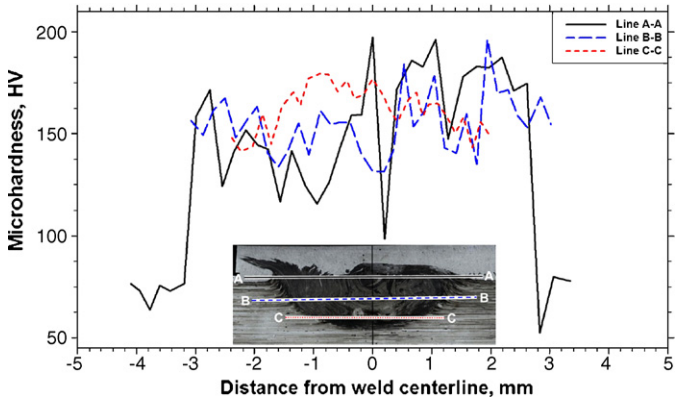

Fig. 9. Hardness measurements in a sample produced using 2500 rpm, and a 0.24 mm plunge depth.

4. Conclusion

The effects of processing parameters on particle dispersion, and hardness were investigated in Al-alloy reinforced with multi-walled carbon nanotubes by friction stir processing. SEM and TEM confirmed that nanotubes were embedded in the lamellae regions of the Al-alloy stir zone and their multi-walled was retained, however evidence was observed that the nanotubes may have fractured during friction stir processing. It was found that increasing the tool rotation speed from 1500 and 2500 rpm and increasing the tool shoulder penetration depth improved the distribution of nanotubes in the Al-alloy matrix. A completely uniform distribution could not be achieved when regularly tangled nanotubes were used as the base material, and it is suggested that multiple passes may be required to further improve the dispersion of nanotubes in the matrix.

Acknowledgements

One of the authors (DKL) is grateful to receive an Undergraduate Student Research Award from the Natural Sciences and Engineering Council (NSERC) of Canada. Financial support from Alberta Finance and Enterprise is also greatly appreciated.

References

[1] T.W. Ebbesen, Annu. Rev. Mater. Sci. 2 (1994) 235–264.
[2] D. Srivastava, C. Wei, K. Cho, Appl. Mech. Rev. 56 (2) (2003) 215–230.
[3] E.T. Thostenson, Z. Ren, T.W. Chou, Compos. Sci. Technol. 61 (2001) 1899–1912.
[4] E.T. Thostenson, C. Li, T.W. Chou, Compos. Sci. Technol. 65 (2005) 491–516.
[5] C. Li, T.W. Chou, Compos. Sci. Technol. 63 (2003) 1517–1524.
[6] C.F. Deng, Y.X. Ma, P. Zhang, X.X. Zhang, D.Z. Wang, Mater. Lett. 62 (2008) 2301–2303.
[7] A.M.K. Esawi, M.A. El Borady, Compos. Sci. Technol. 68 (2008) 486–492.
[8] Y. Morisada, H. Fujii, T. Nagaoka, M. Fukusumi, Mater. Sci. Eng. A 419 (2006) 344–348.
[9] L. Ci, Z. Ryu, N.Y. Jin-Phillipp, M. Rühle, Acta Mater. 54 (2006) 5367–5375.
[10] Q. Pham, S.C. Yoon, C.H. Bok, H.S. Kim, Key Eng. Mater. 345–346 (2007) 1261–1264.
[11] P. Quang, Y.G. Jeong, S.C. Yoon, S.H. Hong, H.S. Kim, J. Mater. Process. Technol. 187–188 (2007) 318–320.
[12] W. Salas, N.G. Alba-Baena, L.E. Murr, Metall. Mater. Trans. A 38 (2007) 2928–2935.
[13] K. Morsi, A. Esawi, J. Mater. Sci. 42 (2007) 4954–4959.
[14] T. Noguchi, A. Magario, S. Fukuzawa, S. Shimizu, J. Beppu, M. Seki, Mater. Trans. 45 (2004) 602–604.
[15] X. Zhang, Y. Shen, C. Deng, D. Wang, L. Geng, Key Eng. Mater. 353–358 (2007) 1414–1417.
[16] R.S. Mishra, Z.Y. Ma, Mater. Sci. Eng. R 50 (2005) 1–78.
[17] Z.Y. MA, Metall. Mater. Trans. A 39 (2008) 642–658.
[18] R.S. Mishra, Z.Y. Ma, I. Charit, Mater. Sci. Eng. A 341 (2003) 307–310.
[19] L.B. Johannes, L.L. Yowell, E. Sosa, S. Arepalli, R.S. Mishra, Nanotechnology 17 (2006) 3081–3084.
[20] R. Nandan, T. DebRoy, H.K.D.H. Bhadeshia, Prog. Mater. Sci. 53 (2008) 980–1023.
[21] M. Guerra, C. Schmidt, J.C. McClure, L.E. Murr, A.C. Nunes, Mater. Charact. 49 (2003) 95–101.
[22] W. Arbegast, in: Z. Jin, et al. (Eds.), Hot Deformation of Al Alloys, vol. III, TMS, Warrendale, PA, 2003, pp. 313–327.
[23] A. Gerlich, P. Su, M. Yamamoto, T.H. North, Sci. Technol. Weld. Join. 11 (1) (2006) 61–71.
[24] A. Gerlich, P. Su, M. Yamamoto, T.H. North, Sci. Technol. Weld. Join. 13 (3) (2008) 254–264.
[25] S. Kazi, L.E. Murr, in: R.S. Mishra, et al. (Eds.), Friction Stir Welding and Processing, TMS, Warrendale, PA, 2001, pp. 139–151.

[26] J.A. Schneider, A.C. Nunes, Metall. Trans. B 35 (2004) 777–783.
[27] Y.S. Sato, Y. Kurihara, H. Kokawa, Proceedings of the 6th International Symposium on 'Friction Stir Welding', TWI Ltd., St. Sauveur, Que., Canada, October 2007.
[28] A. Steuwer, M.J. Peel, P.J. Withers, Proceedings of the 6th International Symposium on 'Friction Stir Welding', TWI Ltd., St. Sauveur, Que., Canada, October 2007.
[29] A. Askari, S. Silling, B. London, M. Mahoney, in: R.S. Mishra, et al. (Eds.), Friction Stir Welding and Processing, TMS, Warrendale, PA, 2001, pp. 43–54.
[30] P. Su, A. Gerlich, T.H. North, G.J. Bendzsak, Metall. Mater. Trans. A 38 (2007) 585–595.
[31] T.M. Keller, M. Laskoski1, M. Osofsky, S.B. Qadri, Phys. Status Solidi A 205 (7) (2008) 1585–1591.
[32] A. Burian, J.C. Dore, H.E. Fischer, J. Sloan, J. Phys. Rev. B 59 (1999) 1665–1668.
[33] H.B. Zhang, G.D. Lin, Z.H. Zhou, X. Dong, T. Chen, Carbon 40 (2002) 2429–2436.
[34] M.W. Mahoney, C.G. Rhodes, J.G. Flintoff, R.A. Spurling, W.H. Bingel, Metall. Mater. Trans. A 29 (1998) 1955–1964.
[35] A. Gerlich, M. Yamamoto, T. Shibayanagi, T.H. North, SAE Technical Series 2008-01-0146.
[36] E.R.I. Mahmoud, K. Ikeuchi, M. Takahashi, Sci. Technol. Weld. Join. 13 (7) (2008) 607–618.